

On the Causes and Dynamics of the Early Twentieth-Century North American Pluvial*

BENJAMIN I. COOK

NASA Goddard Institute for Space Studies, New York, New York

RICHARD SEAGER

Lamont-Doherty Earth Observatory, Palisades, New York

RON L. MILLER

NASA Goddard Institute for Space Studies, New York, New York

(Manuscript received 15 November 2010, in final form 3 March 2011)

ABSTRACT

The early twentieth-century North American pluvial (1905–17) was one of the most extreme wet periods of the last 500 yr and directly led to overly generous water allotments in the water-limited American west. Here, the causes and dynamics of the pluvial event are examined using a combination of observation-based datasets and general circulation model (GCM) experiments. The character of the moisture surpluses during the pluvial differed by region, alternately driven by increased precipitation (the Southwest), low evaporation from cool temperatures (the central plains), or a combination of the two (the Pacific Northwest). Cool temperature anomalies covered much of the West and persisted through most months, part of a globally extensive period of cooler land and sea surface temperatures (SST). Circulation during boreal winter favored increased moisture import and precipitation in the Southwest, while other regions and seasons were characterized by near-normal or reduced precipitation. Anomalies in the mean circulation, precipitation, and SST fields are partially consistent with the relatively weak El Niño forcing during the pluvial and, also, reflect the impacts of positive departures in the Arctic Oscillation that occurred in 10 of the 13 pluvial winters. Differences between the reanalysis dataset, an independent statistical drought model, and GCM simulations highlight some of the remaining uncertainties in understanding the full extent of SST forcing of North American hydroclimatic variability.

1. Introduction

The development of western North America (NA) during the twentieth century was largely made possible through human appropriation of natural water flows for industrial, municipal, and agricultural uses (e.g., Barnett and Pierce 2009; Christensen et al. 2004; Sophocleous 2010; Reisner 1993; Worster 1992). One set of appropriations is legally formalized under the Colorado River Compact (CRC) of 1922 (Christensen et al. 2004;

MacDonnell et al. 1995), an agreement that apportioned discharge from the Colorado River between the states in the Upper (Wyoming, Utah, Colorado, New Mexico) and Lower (California, Arizona, Nevada) Colorado River basins (Christensen et al. 2004). The CRC apportionments are based on an estimated climatological discharge at Lee's Ferry on the Colorado River of 22 billion cubic meters (BCM), using baseline flows from the early twentieth century (Christensen et al. 2004). As development in the West continued, and as the long-term hydroclimate in the West was clarified with longer instrumental records and paleoclimate reconstructions (Fye et al. 2003; Meko et al. 2007; Stockton and Jacoby 1976; Woodhouse et al. 2005), the overly generous nature of the original CRC allocations became apparent. For example, the mean annual discharge at Lee's Ferry calculated over a much longer interval (1906–2000) was only 18.6 BCM, ranging in any given year from 6.5 BCM

* Lamont-Doherty Earth Observatory Contribution Number 7468.

Corresponding author address: Benjamin I. Cook, NASA Goddard Institute for Space Studies, 2880 Broadway, New York, NY 10025.
E-mail: bc9z@ldeo.columbia.edu

to 29.6 BCM (Christensen et al. 2004). The reconstructed discharge extending back to 1512 C.E. is even lower (16.7 BCM), making it highly likely that the flows that formed the basis for the CRC were higher than the hydroclimatic baseline for the last 500 yr (Christensen et al. 2004; Fye et al. 2003; Meko et al. 2007).

The exceptionally high flow during the early twentieth century coincided with anomalous wet conditions throughout the West, spanning approximately 1905–17, a period generally referred to as the early twentieth-century pluvial (the term pluvial referring to wetter than normal conditions) (e.g., Fye et al. 2003, 2004; Woodhouse et al. 2005). This was the most persistent pluvial event in the West to occur during the twentieth century, and recent drought reconstructions based on networks of tree-ring chronologies suggest it may have been the wettest period in the West anytime in the last 1000 yr (Cook et al. 2004). An analysis of temperature and precipitation records from the time suggested that the pluvial (as reflected in river discharge and drought metrics) arose from a combination of anomalously high wintertime precipitation and reduced evaporation from cooler than normal warm season temperatures (Woodhouse et al. 2005).

To date, few studies have discussed the underlying dynamics or causes of the early twentieth-century pluvial. Fye et al. (2004) suggested that anomalously cool temperatures in the North Pacific and warm conditions in the tropical Pacific would have favored increased moisture flux into the Southwest, although this was speculative because of the absence at the time of atmospheric circulation datasets covering this period. Since then, however, new datasets and model simulations have become available, leaving us poised for an in-depth investigation into the causes of the early twentieth-century pluvial in western NA. Here, we use available datasets and an ensemble of general circulation model (GCM) simulations to investigate the North American pluvial (1905–17) and assess 1) the relative importance of temperature versus precipitation for the pluvial moisture surpluses, 2) the dynamics underlying these anomalies, and 3) the importance of sea surface temperature (SST) forcing during this interval.

2. Methods and data

To maintain consistency with previous analyses (e.g., Fye et al. 2004), we define the pluvial interval as 1905–17. Over one of our analysis regions (the central plains), the pluvial moisture surpluses begin several years prior to 1905; the 1905–17 range, however, is the common definition for the pluvial in the literature and this interval includes the major temporal features of the pluvial at the continental scale. Our analysis will use observation-based datasets, proxy-based paleoreconstructions of drought,

and a suite of GCM experiments to investigate the physics and dynamics underlying the spatial structure and temporal evolution of the pluvial event. We divide the West into three regions, distinguished (as shown below) by the main drivers of their respective pluvial moisture surpluses, their own distinct climatologies, and SST–drought teleconnections. Despite these differences, all three regions experienced significant wet conditions during the pluvial. The regions are the Southwest (SW, 25°–42°N, 125°–103°W), the Northwest (NW, 42°–50°N, 125°–103°W), and the central plains (CP, 35°–50°N, 103°–90°W). These regions are outlined later (see Fig. 2 and other subsequent figures).

a. Palmer drought severity index

Droughts and pluvials may be defined in a variety of ways, depending on the research question of interest (Dracup et al. 1980). At the core of all definitions, however, is the concept of a moisture deficit (droughts) or surplus (pluvials). While these surpluses and deficits are typically viewed primarily as a consequence of moisture supply (i.e., precipitation), they may also strongly depend upon evaporative demand. One drought index that incorporates information on moisture supply (via precipitation) and evaporative demand (as a function of temperature) is the Palmer drought severity index (PDSI; Palmer 1965). PDSI is locally normalized around a mean of zero with a typical range of -5 to $+5$; positive values indicate wetter than normal conditions (pluvials) and negative values indicate drier conditions (droughts). PDSI does have some weaknesses. For example, the potential evapotranspiration calculation embedded within the PDSI uses the Thornthwaite equation (Thornthwaite 1948), which uses only temperature as an input; in reality, evapotranspiration may also depend on relative humidity, wind, and cloudiness. Continuous and reliable estimates of these other variables can be difficult to obtain, however, and the significance of these other factors may be largest in energy-limited, rather than moisture-limited, regions with relatively high background relative humidity (e.g., Hobbins et al. 2008). PDSI also does not, in its default form, explicitly model precipitation as snow or accumulated snowpack, which may bias results for regions where seasonal snow cover is an important component of the regional hydrology. Persistence is built into the PDSI calculation, however, meaning that values over one season (e.g., boreal summer) will often partially reflect moisture conditions and climate anomalies from previous months and seasons (e.g., St. George et al. 2010). Summer (June–August, JJA) PDSI, the focus of our analysis, should therefore still contain information regarding temperature and precipitation anomalies during the antecedent winter and spring, in addition to the contemporaneous summer.

We use two different PDSI datasets in our analysis. The first is the *North American Drought Atlas (NADA)* version 2a (information online at <http://www.ncdc.noaa.gov/paleo/pdsi.html>) (Cook et al. 2007), a tree-ring proxy-based reconstruction of PDSI covering much of North America. The *NADA* product reconstructs PDSI for the summer (June–August) season using 1821 tree-ring chronologies, over as many as 286 grid boxes at $2.5^\circ \times 2.5^\circ$ spatial resolution. This product is well validated and versions of the *NADA* have been used in other studies of NA drought variability (Cook et al. 1999, 2004, 2007; Fye et al. 2003; Herweijer et al. 2007). We use the *NADA* to examine the spatial extent and intensity of the pluvial and also place the pluvial anomalies within the context of moisture variability over the last 500 yr.

We also calculate a second set of PDSI values directly from available gridded monthly temperature and precipitation data (see below) in order to investigate the relative contribution of temperature and precipitation to the PDSI during the pluvial. We set the soil moisture capacity for the top and bottom layers to 25.4 mm (1 in.) and 127 mm (5 in.) and use 1926–2000 as our normalization period (“climatically appropriate for existing conditions”). The PDSI calculation is applied to each grid cell’s temperature and precipitation separately; for regional comparisons the new PDSI grids are then spatially averaged over our three defined regions.

b. Temperature and precipitation

Gridded temperature and precipitation data are taken from version 2.1 of the Climate Research Unit (CRU) monthly climate grids (Mitchell and Jones 2005). The CRU data are statistically interpolated from monthly station observations to a regular terrestrial grid at $\frac{1}{2}^\circ$ spatial resolution and monthly temporal resolution, covering the time period 1901–2002. We use these data to look at seasonal temperature and precipitation anomalies during the pluvial and also use them in our own calculation of PDSI. We also use SST data from the Hadley Centre (Hadley Center Sea Ice and Sea Surface Temperature Dataset, HadISST; Rayner et al. 2003) and a dataset of global and hemispherically averaged temperature for the last 150 yr (Hadley Centre–CRU Temperature Anomalies, version 3, HadCRUTv3; Brohan et al. 2006). A measure of the El Niño–Southern Oscillation (ENSO), the Niño-3.4 index, is also calculated from the HadISST dataset. Unless otherwise indicated, all temperature and precipitation anomalies are expressed relative to a 1961–90 climatology. We recognize that there may be issues involved with using this baseline period because of the strong warming trends over the twentieth century. However, we note that 1) this time period is still often used as the standard baseline in climate analyses, 2) data during this

period are relatively well sampled spatially and temporally, 3) persistent drought or pluvial events over NA are generally absent during this interval, and 4) it is difficult to develop a comprehensive baseline prior to the pluvial period and major warming trends.

c. Atmospheric circulation

Data on atmospheric circulation and dynamics are taken from the Twentieth Century Reanalysis Project (20CR; Compo et al. 2006, 2011; Whitaker et al. 2004). This product covers the time span 1871–2008, using a data assimilation model forced by observed climate forcings and SSTs (from HadISST). This reanalysis only assimilates surface and sea level pressure observations, and versions of the 20CR have already been used to investigate early twentieth-century circulation features (e.g., Cook et al. 2011b; Wood and Overland 2009). Because the reanalysis is constructed using an ensemble approach, a useful indicator of uncertainty is the ensemble spread in the variables, for example in annual averaged 500-hPa heights (Fig. 1). The ensemble spread is low where the reanalysis is tightly constrained by either a high density of observations (e.g., North America and Europe) or the prescribed SST forcing (e.g., the tropics, where SST forcing of the atmosphere is strong). Over our region of interest, the Pacific–North American sector, the spread is on the order of 20–40 m over the land, but much higher over the North Pacific. This is not too surprising, given the relative paucity of observations available in the North Pacific during this time. Despite these caveats, we feel the 20CR is still an appropriate choice for our analysis, given the relatively low ensemble spread over NA and our use of the 20CR as supporting analysis to our main points.

d. GCM experiments

We also use results from a 16-member ensemble of atmosphere GCM simulations forced with observed SSTs to determine the extent to which SST forcing may be able to explain climate anomalies during the pluvial. These simulations cover 1856 to the near present, and have been previously used to investigate SST forcing of drought over NA with good success (Seager et al. 2005b; Seager 2007). The SST forcing comes from Kaplan et al. (1998) for the tropical Pacific Ocean for the entire period and, where available, for 1856–70, and from the Hadley Centre (Rayner et al. 2003) outside of the tropical Pacific from 1871 on. The GCM is the Community Climate Model version 3 (CCM3), developed at the National Center for Atmospheric Research (NCAR; Kiehl et al. 1998). The model runs are referred to as GOGA for Global Ocean Global Atmosphere. All results shown are the mean of a

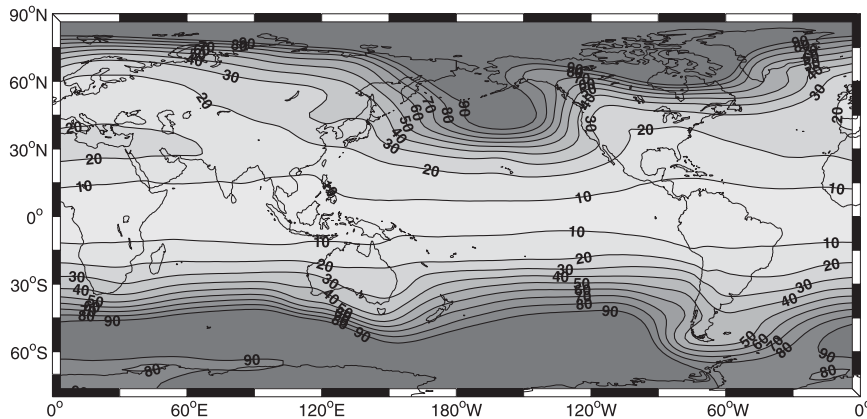


FIG. 1. Ensemble spread (m) in annual average 500-hPa geopotential heights from the 20CR during the pluvial interval (1905–17).

16-member ensemble, representing the SST-forced component of the model variability.

3. Results and discussion

a. The pluvial within a long-term context

Anomalous wet conditions were widespread throughout western NA during the pluvial, with positive tree-ring-reconstructed PDSI anomalies spanning from Mexico to southern Canada and from the Pacific coast across the Great Plains (Fig. 2). The largest PDSI anomalies (+3 and greater) are concentrated along an axis extending from the SW into the NW and northern CP regions. Notably, there are no major drought conditions ($\text{PDSI} < -1$) anywhere during this time period, at least in the multi-year average.

All three regions are characterized by high moisture variability and persistent drought and pluvial periods over the last 500 yr (Fig. 3); time series are smoothed (5-yr low-pass filter) to emphasize persistent events. Twentieth-century drought events are well resolved by the PDSI anomalies, including the well-documented droughts in the 1950s (SW) and the 1930s' "Dust Bowl" (NW and CP), as well as the multidecadal "megadroughts" in previous centuries. Compared to other pluvial intervals over the last 500 yr, the early twentieth-century event generally stands out through a combination of its intensity, duration, and spatial extent. In all three regions, the time evolution of the pluvial indicates two wet phases, with a break toward dry or near-normal conditions around 1910. The break in 1910 corresponds to La Niña conditions in the tropical Pacific, a situation that typically suppresses precipitation in SW NA and the southern Great Plains. Over the CP region, the pluvial appears to have started earlier than in either the SW or NW, and the post-1910 phase of the pluvial also appears weaker (drier) in this region.

b. Temperature and precipitation during the pluvial

Temperature anomalies were generally cool throughout the West, especially during the spring (March–May, MAM) and summer (JJA) peak evaporative seasons (Fig. 4). The West was also cooler than normal during winter (December–February, DJF), with the exception of slightly warmer than normal conditions over California. The largest positive precipitation anomalies occurred in the SW during DJF, with increases on the order of 50%–60% (Fig. 5), and in the SW during MAM, although the spring anomalies occur over a much more limited area. There are some minor increases over the region of the North American monsoon, defined here as the areas of Mexico and the Southwest that receive $>50\%$ of their annual precipitation during the boreal summer (roughly 22° – 32°N and 112° – 104°W) (Adams and Comrie 1997). In the SW regional average, however, these limited positive anomalies during JJA are largely canceled out by the negative anomalies farther west. During DJF

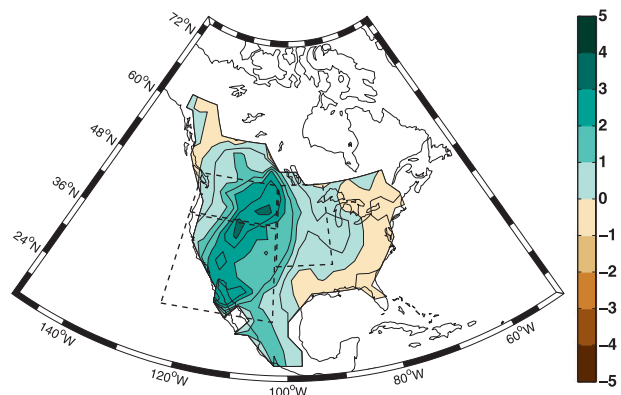


FIG. 2. Summer season (JJA) tree-ring-reconstructed PDSI anomalies from the NADA, averaged across all pluvial years (1905–17).

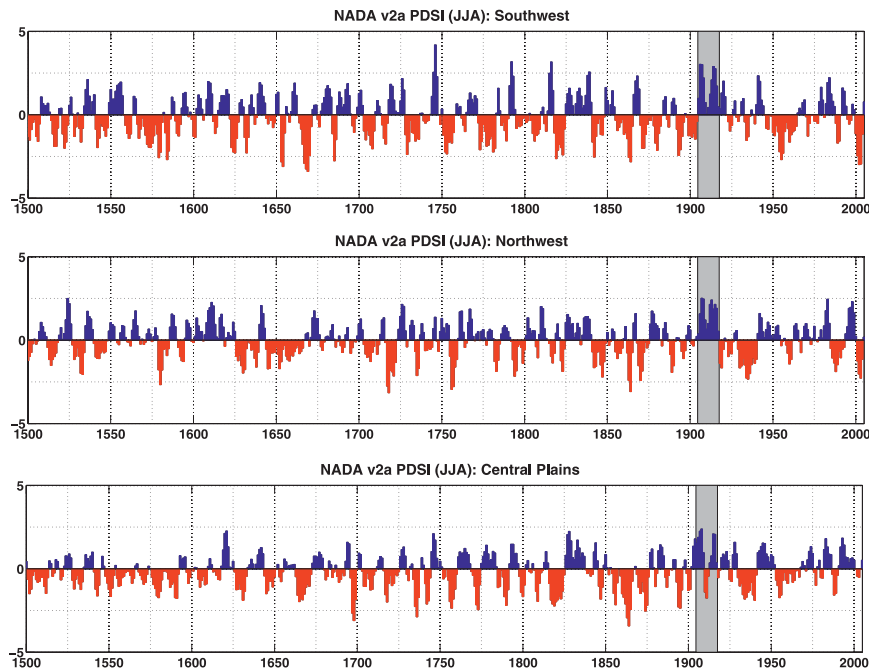


FIG. 3. Area-averaged summer season (JJA) tree-ring-reconstructed PDSI from the *NADA* v2a for 1500–2005. All time series are smoothed with a 5-yr low-pass filter. Time series correspond to the outlined boxes in Fig. 1: the Southwest (SW; 25°–42°N, 125°–103°W), the Northwest (NW; 42°–50°N, 125°–103°W), and the central plains (CP; 35°–50°N, 103°–90°W).

there were also wet anomalies in the CP, but these were relatively low in absolute terms because the annual cycle in precipitation over this region peaks in the summer. What may be even more remarkable is how many regions experienced precipitation deficits during the pluvial, especially the SW during JJA and autumn (September–November, SON), the NW during DJF, and the CP during MAM. This supports the hypothesis (Woodhouse et al. 2005) that cool temperature anomalies and low evaporative demand may be as important as precipitation for explaining the large moisture surpluses reflected in the positive PDSI values.

A look at the actual temperature (K) and precipitation (mm day^{-1}) anomalies averaged over the three regions during the pluvial provide some further insight (Fig. 6). Overlain in the precipitation plots is a scaled-down (60%) version of the Niño-3.4 index (dashed line). When Niño-3.4 is strongly positive, this is indicative of warm-phase El Niño events generally associated with increased winter and spring precipitation in the Southwest and decreased precipitation during the same seasons in the Northwest. During the pluvial, there were five significant ($\geq +0.5$ standard deviation from the mean) El Niño events: 1905, 1906, 1912, 1914, and 1915.

The main evaporative season in all three regions is summer (JJA), and all regions show fairly consistent cool anomalies throughout the pluvial during this season

(Fig. 6, left). In the SW, only 1910 is marginally positive, and the remaining years are all negative, with anomalies on the order of -0.5 to -1 K. Absolute anomalies are even cooler in the NW, matching or exceeding -1 K in five of the pluvial years. In the CP, the cool anomalies start before 1905, averaging about -2 K, and continuing until 1908 with anomalies of about -1 K, coinciding with the earlier start of the pluvial in this region. Afterward, temperature anomalies are a bit more equivocal, with some major cool years (1912, 1915) but, otherwise, near-normal temperatures. Over the SW and NW, the major precipitation season is DJF; over CP the annual precipitation peaks during JJA (Fig. 6, right). Our SW region, as defined, does include some areas with significant summer precipitation, especially regions associated with the North American monsoon. Summer precipitation anomalies over the SW during the pluvial are muted relative to the anomalies during DJF, however, and we also note that we do explicitly account for any summer precipitation changes in our PDSI sensitivity analysis (see below). In the SW, there were major positive precipitation anomalies during both the early and later stages of the pluvial; this contrasts with the NW, which showed some minor increases in the beginning but, overall, negative precipitation anomalies throughout. Remarkably, only two of the major precipitation years (1914 and 1915) in the SW actually correspond to El Niño events, despite

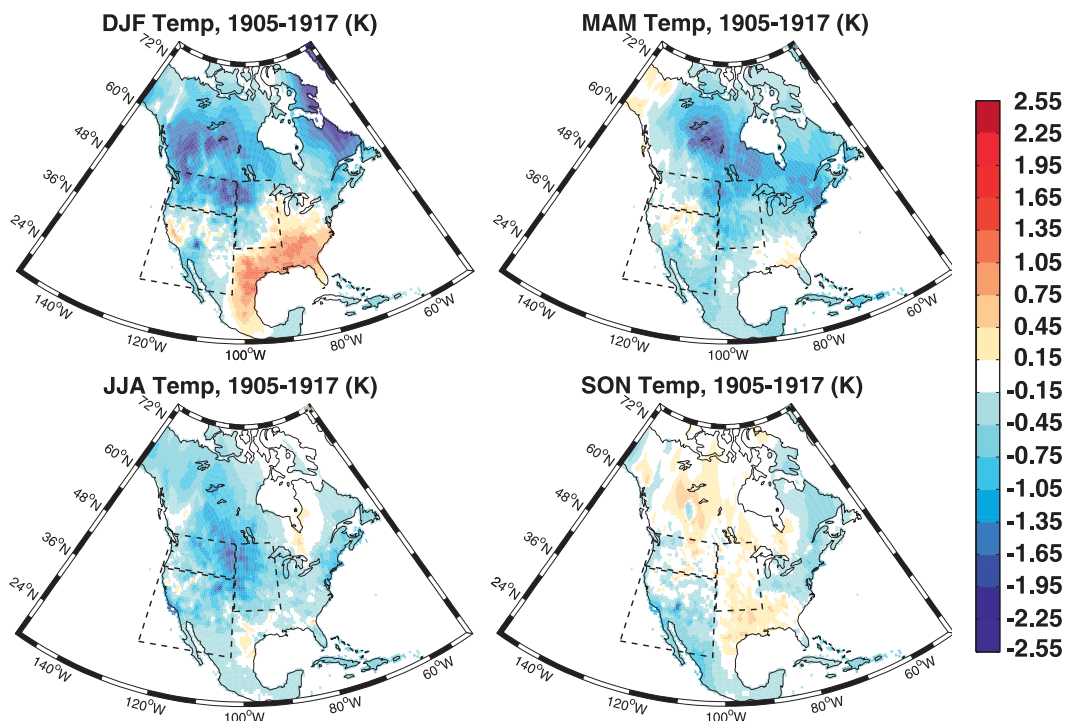


FIG. 4. Seasonal temperature anomalies during 1905–17 from the CRU 2.1 climate grids, relative to the 1961–90 mean (K).

the significant correlation between Niño-3.4 and precipitation over the SW during DJF (Pearson's $r = +0.33$). Our SW region includes some areas where the El Niño–precipitation teleconnections are strongest during the spring and autumn (Andrade and Sellers 1988) rather than winter, and we do find wet spring (MAM) anomalies in other El Niño years during the pluvial (1905, 1906, 1912), although these are muted relative to DJF (not shown). As with the cool temperature anomalies, the positive precipitation anomalies in the CP begin before 1905. These precipitation anomalies persist through the first 4 yr of the pluvial; after 1908 the CP experiences precipitation deficits every year except for 1915.

c. PDSI: Temperature versus precipitation

To what extent were the moisture surpluses during the pluvial, as reflected in PDSI, a consequence of enhanced precipitation versus reduced evaporative demand from cool temperature anomalies? To answer this question, we calculate our own PDSI using temperature and precipitation data from the CRU climate grids, spatially averaging over the three regions (Fig. 7, top). Mean PDSIs calculated over the entire pluvial interval are +0.83, +0.73, and +0.33 for the SW, NW, and CP, respectively. We expect our calculated PDSI to differ somewhat from the values in Fig. 3, as the *NADA* PDSI represent a statistical scaling using tree growth as a

proxy rather than the direct calculation we conduct here. The calculated PDSI is generally quite similar to that of the *NADA*, showing the two-phase nature of the pluvial (pre- and post-1910) in all three regions and the early start to the pluvial over the CP.

To test the importance of temperature versus precipitation as a contributing factor to summer PDSI during the pluvial, we alternately substitute climatological values (1961–90) instead of the observed temperature and precipitation into the PDSI calculation. We substitute climatological values for each month (January–December), rather than specific seasons, to account for minor but potentially important contributions from anomalies outside the main precipitation and evaporation seasons. Substituting climatological temperature (keeping observed precipitation) into the PDSI calculation results in varying impacts across the three regions (Fig. 7, center). The average pluvial PDSI for the SW decreases moderately to +0.60, but PDSI during the major pluvial years (1905, 1906, 1907, 1912, 1914, and 1915) is only slightly diminished. Over the NW, there are major reductions in PDSI across most pluvial years, with mean PDSI dropping by over half from +0.73 to +0.31. Even more dramatically, mean PDSI switches from positive to negative over the CP (+0.33 to −0.15), suggesting that, without the cool temperatures, there would have been drought conditions over this region. Calculations with climatological precipitation

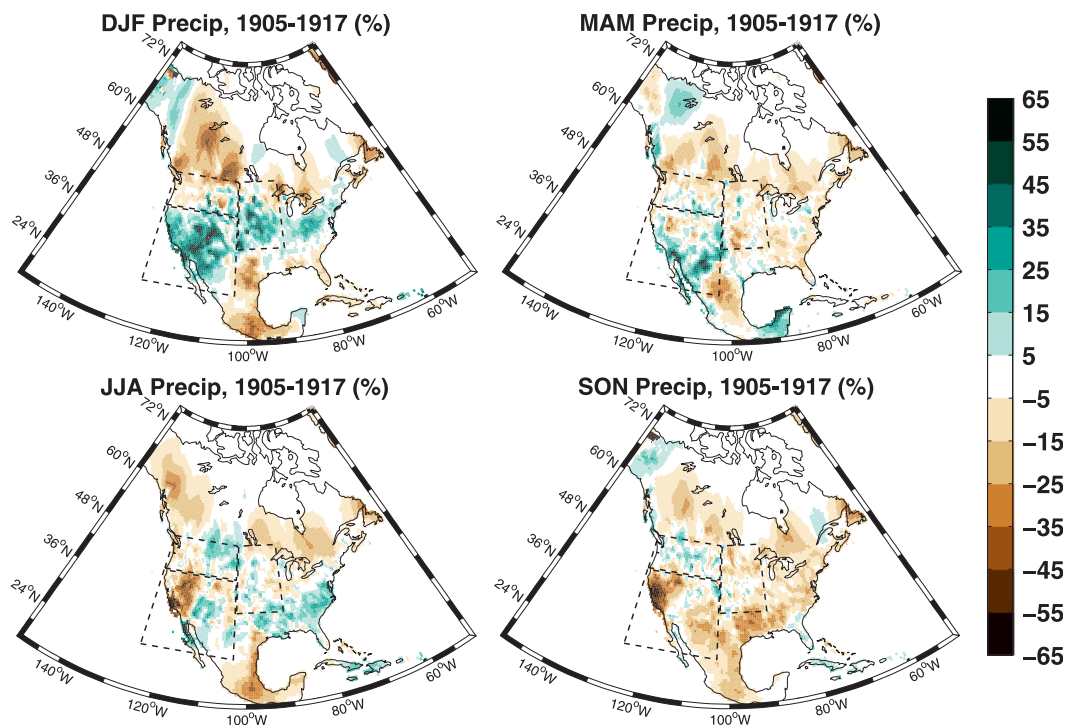


FIG. 5. Precipitation anomalies during 1905–17 from the CRU 2.1 climate grids, expressed as a percent difference relative to the 1961–90 mean.

and observed temperatures (Fig. 7, bottom) reduce the original calculated PDSI in the SW by 62% to +0.33. In the NW, the mean PDSI is reduced to +0.66, a relatively muted response compared to the climatological temperature scenario, but with the major pluvial years (1907, 1912, 1916) reduced by half. In the CP, substitution of climatological precipitation actually enhances the pluvial, increasing mean PDSI to +0.84, muting early PDSI anomalies slightly but completely eliminating the later drought years during the second half of the pluvial. From these results we conclude that the causes of the moisture surpluses varied across these three regions, driven by high precipitation (SW), low evaporative demand (CP), or a combination of both (NW).

Cool temperature anomalies, and the accompanying low evaporative demand, appear to be important for explaining the pluvial moisture surpluses. However, this explanation depends on the cool temperatures being an independent factor and not arising from their occurrence near the beginning of the twentieth-century warming trends or a result of increased precipitation, which would make things wet and cool by favoring latent over sensible heating or increasing cloud cover and shortwave reflection. In the first case, our cool temperatures would simply be a consequence of our relatively warm baseline; if the latter case were true, this would mean the temperature anomalies would be a covariate with the precipitation, rather than

an independent causal factor. A look at global and hemispheric temperatures for the late nineteenth to early twentieth centuries shows that temperature anomalies during the pluvial period were cool even relative to previous decades (Fig. 8). Thus, an observer in 1920, looking back, and with no knowledge of the coming warming, would have characterized the pluvial decade as anomalously cool compared to previous years. For all three regions there is a significant ($p < 0.05$, calculated over 1901–2002) negative relationship between precipitation and temperature (Fig. 9). However, when the pluvial years are isolated (blue dots), we see that temperatures are near normal or cool (left side of the dashed line), regardless of the precipitation anomalies. Because precipitation during the winter and spring may be stored as snowpack that carries over into subsequent seasons, the temperature response to precipitation may also be lagged by several months. We repeated the correlation analysis, this time comparing JJA temperature against antecedent DJF and MAM precipitation. For this lagged analysis, only the SW showed a significant correlation (MAM precipitation versus JJA temperature: $\rho = -0.23$, $p < 0.05$), and with similar results indicating cool temperatures during the pluvial that were largely independent of the precipitation anomalies. This gives strong evidence to reject the second explanation and conclude that the temperature anomalies during the pluvial were largely

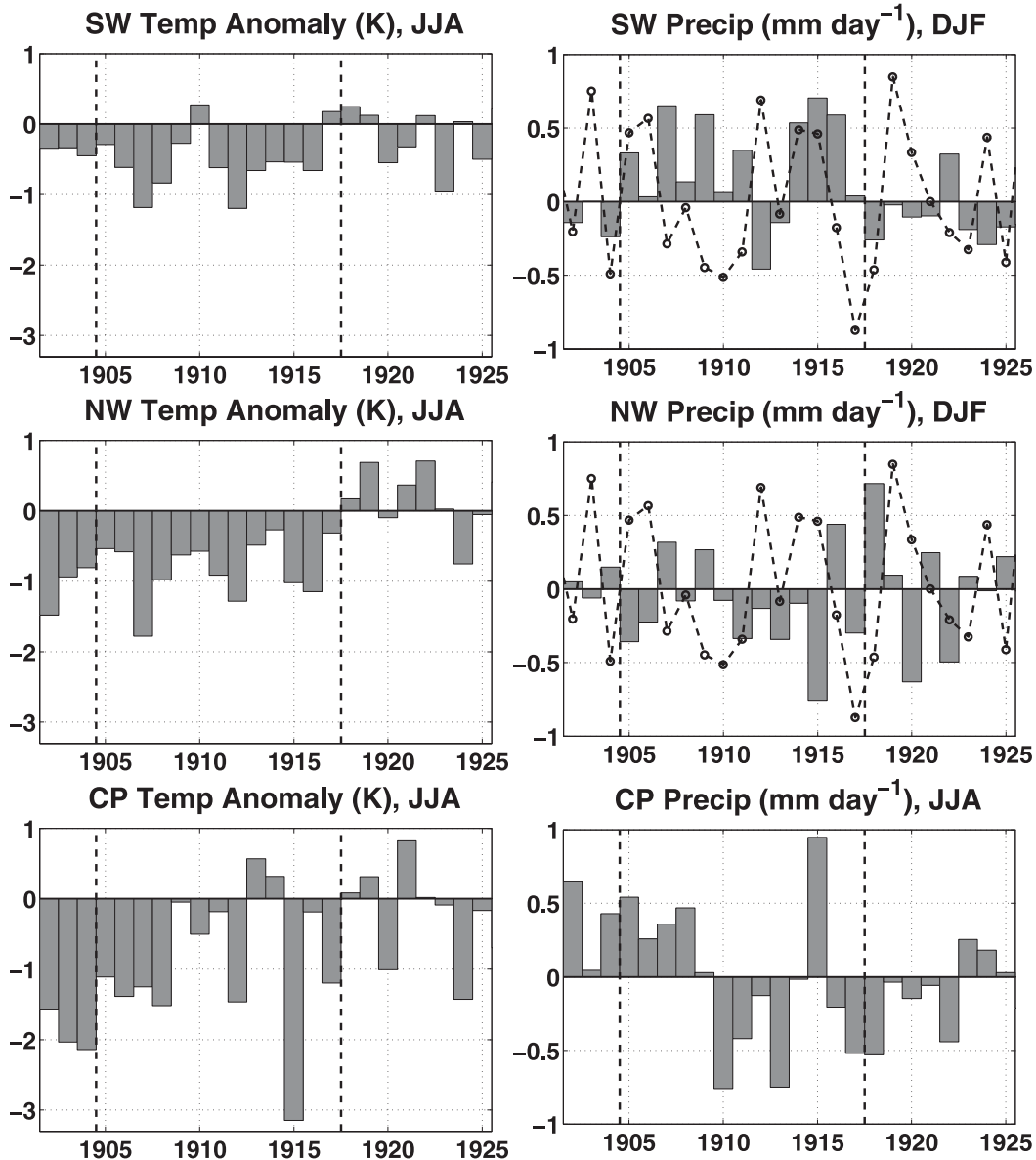


FIG. 6. Temperature (K) and precipitation (mm day^{-1}) anomalies during 1905–17 for the three outlined regions. The indicated 3-month seasons represent the main evaporation and precipitation seasons for each region. Dashed lines are a scaled version of the Niño-3.4 index, included to indicate the five El Niño years during the pluvial (1905, 1906, 1912, 1914, and 1915). All temperature and precipitation anomalies are relative to the 1961–90 mean.

independent from the precipitation anomalies, allowing them to be an independent causal factor for the pluvial moisture surpluses.

d. Sea surface temperatures

Drought and pluvial events over western NA are largely modulated by variations in SSTs, originating primarily from the tropical Pacific (Seager et al. 2005b), part of a zonally and hemispherically symmetric pattern of global hydroclimatic variability (Seager et al. 2003, 2005a).

Increased precipitation in the SW is associated with warm-phase El Niño events while cold-phase La Niña events typically suppress precipitation over the same region. The sign of the ENSO–precipitation teleconnections is reversed in the NW, with El Niño events leading to drier than normal conditions. The influence of the tropical Pacific is typically strongest during boreal winter.

Composited DJF SST anomalies from all El Niño events (defined as the Niño-3.4 index $\geq +0.5$ standard deviation) over the last 130 yr are shown in the top panel

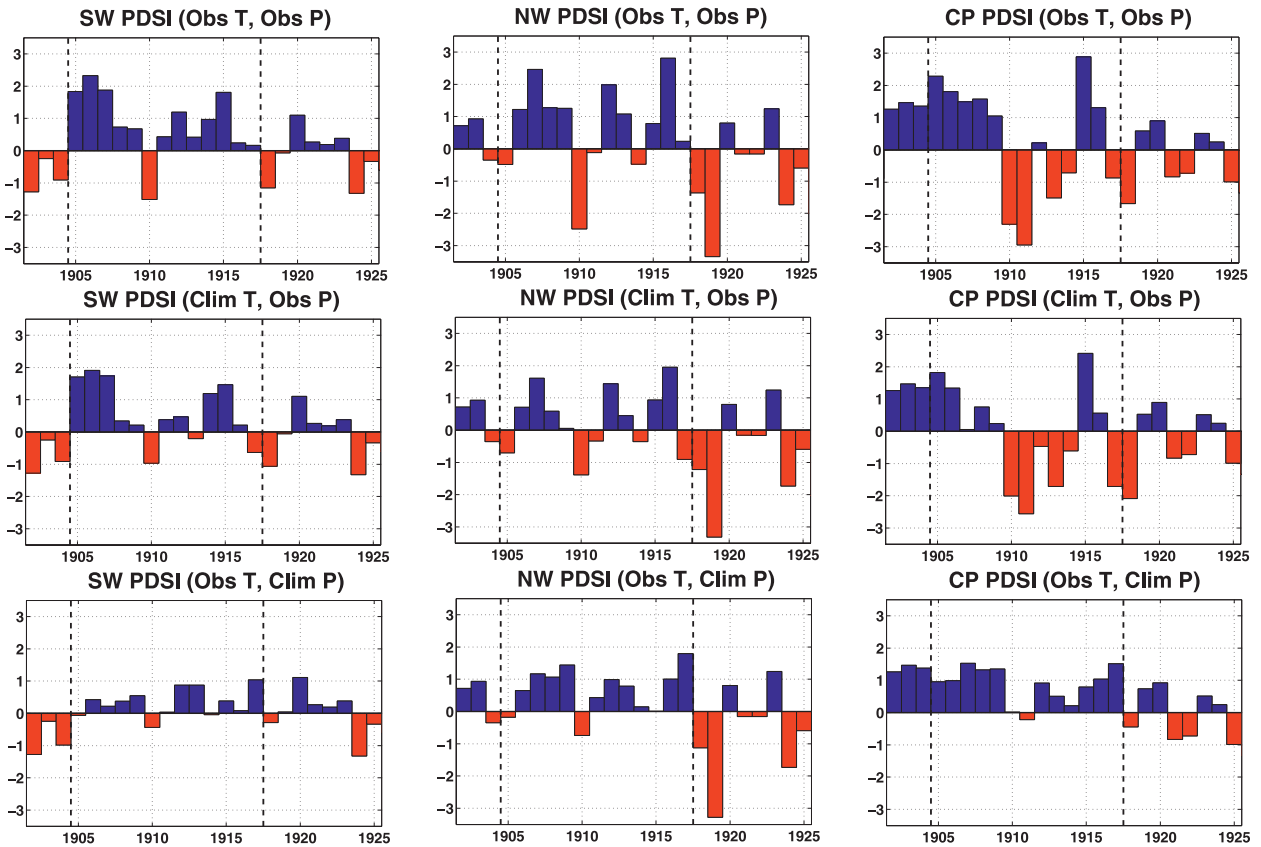


FIG. 7. Summer season (JJA) PDSI calculated from the CRU 2.1 precipitation and temperature climate grids averaged over the (left) SW, (middle) NW, and (right) CP. For the pluvial period (1905–17), PDSI is alternately calculated with (top) observed temperature and observed precipitation, (middle) climatological temperature and observed precipitation, and (bottom) observed temperature and climatological precipitation.

of Fig. 10. During a typical El Niño event, warm SST anomalies extend across most of the tropical Pacific, flanked by cool SSTs in the extratropical central North and South Pacific Ocean basins. Warm SSTs also typically occur in a narrow band along the west coast of NA. Averaged across all years during the pluvial, SSTs were globally cooler than normal (Fig. 10, bottom) and the tropical Pacific is near normal, despite the occurrence of five El Niño events (1905, 1906, 1912, 1914, 1915). Even during the pluvial El Niño events, off-equatorial SST anomalies in the Pacific deviate from the expected El Niño pattern, especially in the extratropical North Pacific, which was nearly universally cool across the entire basin (not shown). Coupled with the major precipitation surpluses in the SW during off El Niño years, this suggests that El Niño forcing may be insufficient to satisfyingly explain the full pluvial anomalies. The North Atlantic was also cooler than normal during the pluvial, a condition that is typically associated with increased precipitation in central NA, especially during the warm season (Enfield et al. 2001; Kushnir et al. 2010; Mo et al. 2009).

e. Dynamics

The impacts of various modes of climate variability and atmospheric circulation on climate in western NA are well established, including the Pacific–North America pattern (PNA) (Wallace and Gutzler 1981), the Arctic Oscillation (AO) (Hu and Feng 2010; McAfee and Russell 2008), and ENSO (Andrade and Sellers 1988). What is less clear, however, is the extent to which the circulation during the pluvial or other intervals represents a forced response to SSTs versus internal atmospheric variability, an important distinction as SSTs currently provide the best source of predictability for NA hydroclimate (Schubert et al. 2008, 2009). Forcings from tropical Pacific and tropical Atlantic SSTs are currently well constrained by numerous studies (e.g., Cook et al. 2011a; Kushnir et al. 2010; Seager et al. 2005b) but the role of extratropical SSTs, especially in the extratropical Pacific, is still controversial. There is limited empirical and modeling evidence suggesting that SSTs in the extratropical Pacific may influence the overlying atmosphere

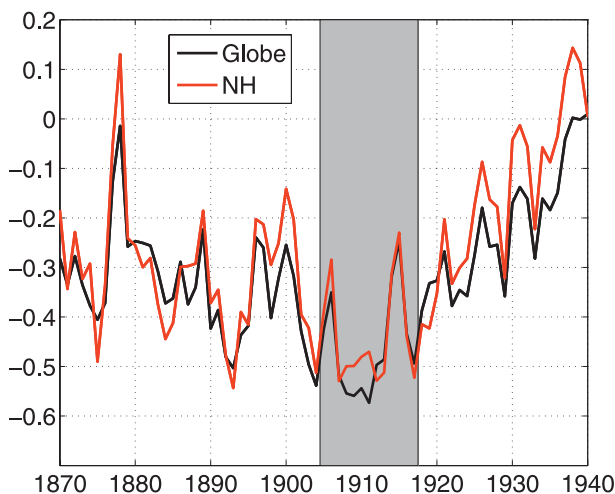


FIG. 8. Global and Northern Hemisphere averaged surface temperature anomalies (K, from HadCRU), for 1870–1940. The 1905–17 pluvial interval (shaded gray) was relatively cool compared to either the preceding or following decade.

(Frankignoul and Sennéchael 2007; Kushnir et al. 2002; Peng and Whitaker 1999; Wen et al. 2010). Many of the most recent studies suggest that warm SSTs in the Kuroshio extension region may force or reinforce an upper-level ridge near the Gulf of Alaska during boreal winter, with the atmospheric response typically lagging the ocean by 4–5 months (Peng and Whitaker 1999; Frankignoul and Sennéchael 2007; Wen et al. 2010). Discerning the magnitude and significance of the forced response is difficult, however, due to the high internal variability in the atmosphere, the fact that extratropical Pacific SST variability is not independent from ENSO, and the importance of the atmosphere as the primary driver of SST variability in the extratropics (Deser et al. 2010; Junge and Haine 2001; Kushnir et al. 2002).

Winter (DJF) circulation during the pluvial, as reflected in the 500-hPa geopotential height anomalies, is

characterized by negative anomalies off the west coast of NA, flanked by positive heights over the western extratropical Pacific and over eastern NA (Fig. 11, top). This configuration favors increased moisture advection into the SW along a southwesterly track, a pattern highly favorable for so-called Pineapple Express wintertime storm events (Dettinger 2004; Fye et al. 2004). This circulation pattern bears some superficial similarities to the canonical circulation response to El Niño forcing, but with some substantial differences (Fig. 11, middle). Specifically, the negative height anomalies are weaker and shifted eastward, while the positive heights over NA shift southeast, extending over eastern NA and Mexico. The apparent weak circulation response to ENSO during the pluvial is consistent with the limited impact of ENSO on the precipitation in the SW during DJF and MAM, described previously. The circulation pattern also diverges from the expected warm SST ridge–cold SST trough response that would be expected given the cold North Pacific SSTs (Peng and Whitaker 1999; Frankignoul and Sennéchael 2007; Wen et al. 2010). Low-level height anomalies over the subtropical North Atlantic are weak (<5 m) or nonexistent during MAM and JJA (not shown). The absence of significant high pressure anomalies over this region suggests a negligible role for cold North Atlantic SSTs in forcing the precipitation anomalies.

We calculated the AO index in the 20CR using the leading mode of the monthly mean wintertime sea level pressure following the definition of Thompson and Wallace (1998). The AO index from the 20CR correlates well (Spearman rank correlation, $r = 0.98$, 1949–2008) with the same index calculated from the National Centers for Environmental Prediction (NCEP)–NCAR reanalysis (Kalnay et al. 1996). Spatial expression of the AO is similar in both datasets, with positive departures (defined as plus one-half standard deviation from the mean) in the AO index during boreal winter (DJF)

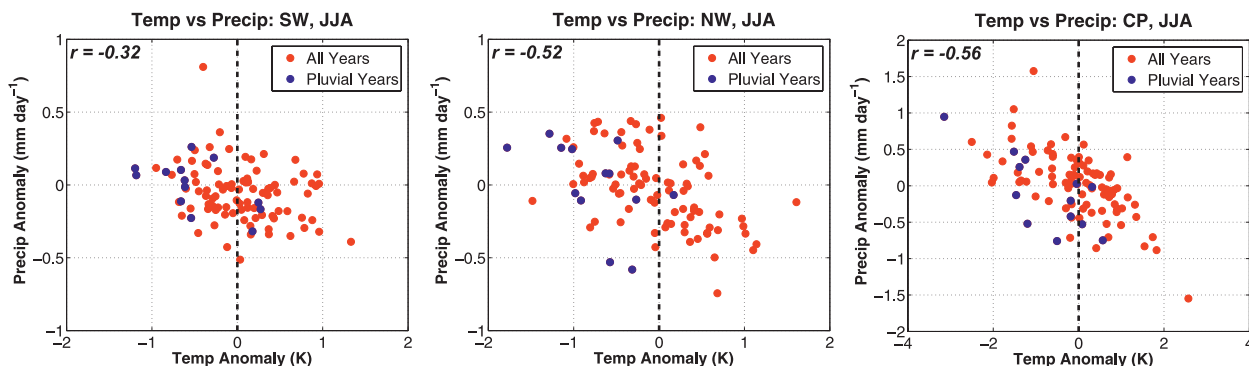


FIG. 9. Summer (JJA) temperature vs precipitation anomalies, averaged over the three regions for 1901–2002 (from the CRU 2.1 climate grids). Years during the pluvial (1905–17) are colored in blue. Spearman rank correlations between temperature and precipitation are shown in each plot.

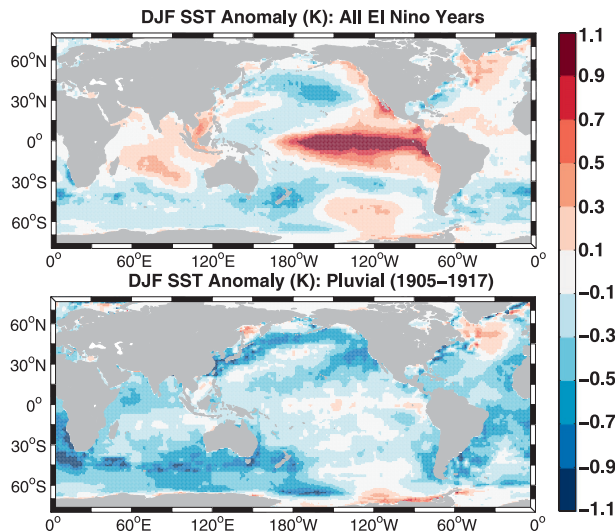


FIG. 10. (top) Composite DJF SST anomalies (K, from HadISST v1) from all El Niño years ($n = 38$) during the instrumental period compared to (bottom) mean composite SST anomalies from the 13-yr pluvial interval (1905–17).

characterized by positive height anomalies in the mid-latitudes and negative height anomalies over the Arctic (not shown). Over the Pacific–North America sector (Fig. 11, bottom), this manifests itself primarily as positive heights over the North Pacific and eastern NA, flanking negative heights over northwestern NA. In 10 of the 13 yr composing the pluvial does the +AO index coincide with departures during DJF (1905, 1906, 1907, 1908, 1909, 1910, 1911, 1913, 1914, and 1916), and the imprint of these +AO events can be clearly seen (Fig. 11, top). In particular, the positive height anomalies over the western North Pacific and eastern NA during the pluvial match the location and magnitude of the +AO composite anomalies. Temperature and precipitation anomalies associated with the +AO composite also show features that are highly consistent with anomalies during the pluvial (Fig. 12). Temperatures over eastern NA are warmer than normal during +AO winters and colder over northeastern Canada and the Northwest; these features are present during the pluvial, although the warming is over a more restricted area than would be predicted from the AO alone. In addition, +AO winters are associated with modest increases in precipitation stretching from the Southwest, across the central plains, and into eastern NA just south of the Great Lakes region. Positive precipitation anomalies occur over this same geographic band during the pluvial. It should be noted that, in a previous study, McAfee and Russell (2008) described a minor and largely insignificant relationship between the AO and precipitation in the West during boreal winter, apparently at odds with the analysis described here. We note, however, that this

previous study used a different precipitation dataset, conducted their analysis over a much shorter temporal interval, and employed a different season for their AO index calculation (January–March, JFM). Repeating their analysis as best we could (JFM AO from 20CR versus DJF precipitation from CRU), we were able to largely reproduce their results. Given the methodological differences between this study and McAfee and Russell (2008), we feel confident that our own analysis and interpretation of the AO impacts on precipitation in western NA is correct.

f. Modeling

The AO appears to be an important driver of the pluvial temperature and precipitation anomalies during DJF, with El Niño also playing a limited role in the precipitation and circulation anomalies during DJF and MAM. To understand the extent to which the pluvial climate anomalies represent a response to external forcing (e.g., SSTs) versus internal atmospheric variability, we leverage the GCM simulations described previously to look at the climate response over NA to global observed SSTs during the pluvial. Because the AO is primarily an internal atmospheric mode of variability, we do not expect that the model will be able to reproduce the +AO events and related circulation features during the pluvial. However, the model may be able to resolve atmospheric responses to SST forcing originating from the extratropical Pacific, as other studies have attempted to do (Frankignoul and Sennéchaël 2007; Kushnir et al. 2002; Peng and Whitaker 1999; Wen et al. 2010).

Geopotential heights composited from all El Niño years in the GCM ensemble show that the model does a good job reproducing the major circulation features associated with El Niño in the reanalysis (Fig. 13, top), although with somewhat weaker amplitudes. During the pluvial, however, the height anomaly pattern diverges from the reanalysis and seems to simply reflect the imprint of the five El Niño events (Fig. 13, bottom). In the model composite, the positive height anomalies over the western North Pacific and eastern NA are absent, and the major region of negative heights is centered over the ocean, rather than being shifted to the east over the west coast of NA as it is in the reanalysis. Since these features were largely a consequence of the +AO during the pluvial, something the model is not capable of reproducing as a response to SST forcing, these differences are not surprising. Temperature anomalies from the GCM ensemble (Fig. 14) are cool but muted compared to the observations and the model also does not reproduce the observed spatial structure. The precipitation anomalies from the model largely reflect the influence of El Niño events in the

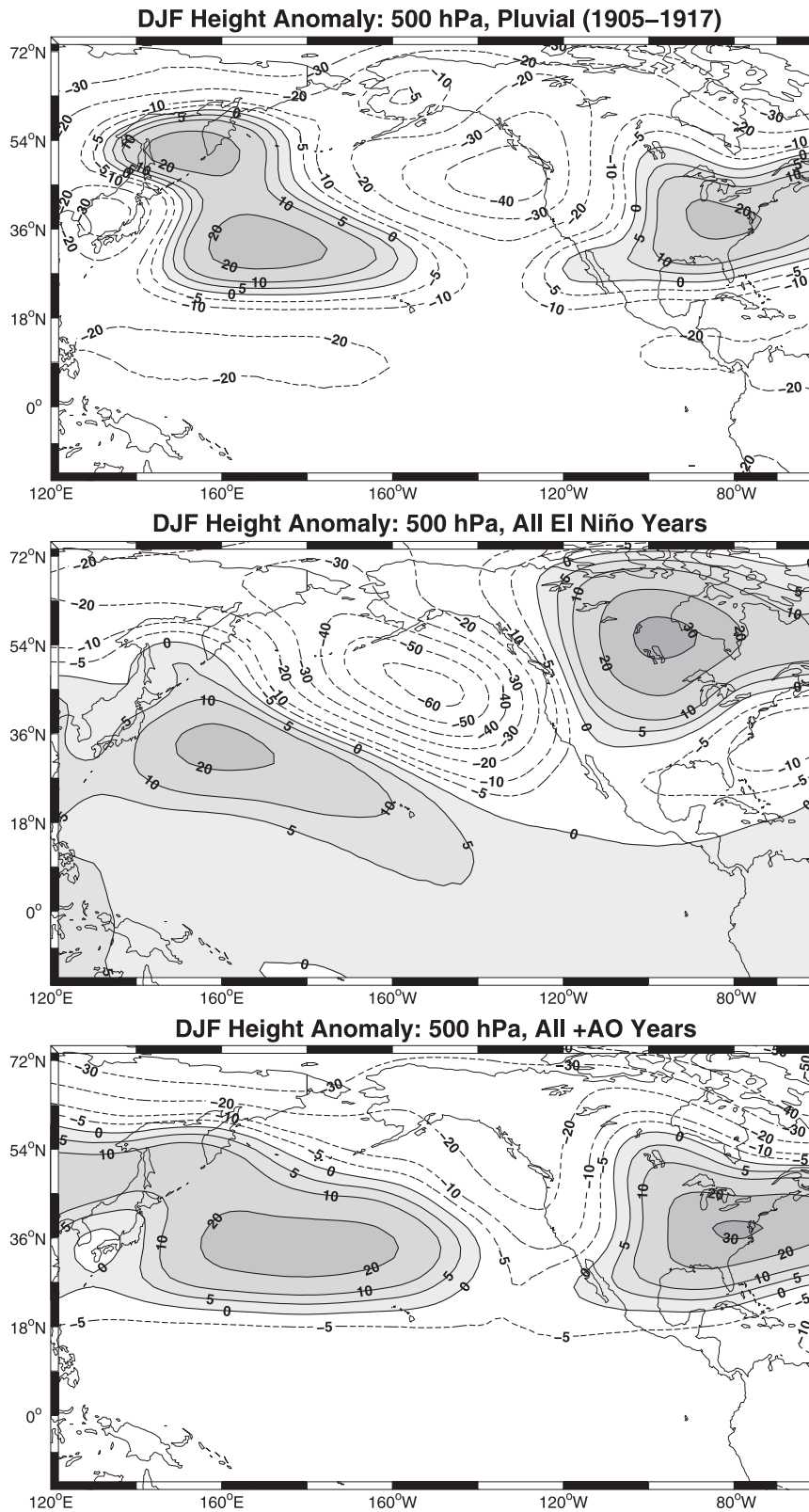


FIG. 11. Composite 500-hPa geopotential heights (m) for all (top) pluvial years (1905–17), (middle) composite El Niño winters, and (bottom) composite +AO winters.

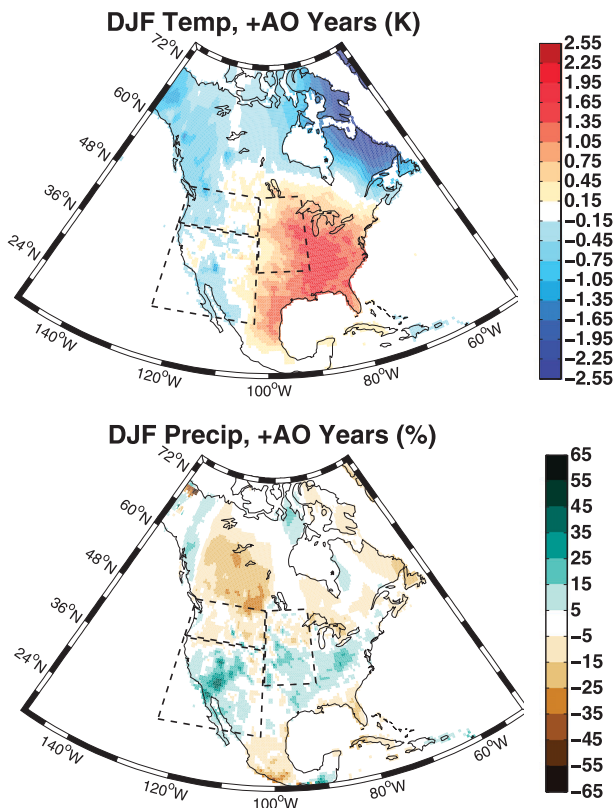


FIG. 12. Composite temperature and precipitation anomalies for all +AO winters.

mean pluvial circulation, with enhanced precipitation in the SW and Mexico in DJF and MAM (Fig. 15). These anomalies, however, are muted compared to the observations (Fig. 5), and have slightly different spatial patterns. For example, model precipitation anomalies during DJF are shifted too far to the south, and the major precipitation increases occur in MAM, rather than DJF. These deviations from the observed anomalies are also not surprising in light of the potentially important impact of the +AO during the pluvial. As an aside, it should also be noted that two other atmosphere circulation models, versions 3 and 4 of the Community Atmosphere Model, CAM3 and CAM4, respectively, are also unable to reproduce the pluvial anomalies (information online at <http://rainbow.ideo.columbia.edu/%7Ejennie/comparemodel/>).

In a recent study, Cook et al. (2011a) used a statistical drought model to investigate the SST forcing of persistent multiyear twentieth-century hydroclimatic events over western NA, including the pluvial. Using statistical modes representing drought variability associated with tropical and extratropical Pacific SSTs, they were able to reproduce the magnitude and spatial pattern of the pluvial above random noise in over 95% of their model ensemble members, with an anomaly correlation between

the ensemble median modeled drought pattern and observations of 0.76. Their conclusion, that knowledge of tropical and extratropical Pacific SSTs should be sufficient to predict the pluvial, appears to be at odds with results from our SST-forced GCM simulations which seem unable to fully resolve the important circulation and precipitation anomalies.

In the statistical model, the mode of drought variability associated with the extratropical North Pacific SSTs may simply reflect forcing of SSTs by atmospheric circulation anomalies, or could be a high-latitude expression of ocean variability linked to dynamics in the tropical Pacific (An et al. 2007; Schneider and Cornuelle 2005). This would cause internal variability to be mistaken for forcing in the statistical model and overestimate the SST-forced component of the pluvial. On time scales longer than ENSO, Pacific SST variability is dominated by the Pacific decadal oscillation (PDO), or Pacific decadal variability (PDV), which has a strong expression in the North Pacific Ocean (Mantua et al. 1997; Zhang et al. 1997). Much work has been done, mostly of an observational nature, suggesting that NA hydroclimate can be influenced by the PDO (e.g., Gershunov and Barnett 1998; Goodrich 2007; McCabe et al. 2004, 2008). For example, differences in a variety of hydroclimatic variables can be seen in western NA between positive and negative phases of the PDO, even when only neutral ENSO years are considered (e.g., Goodrich 2007). And for various combinations of PDO and ENSO phases, drought and pluvial anomalies can be either amplified or diminished (e.g., Kurtzman and Scanlon 2007). However, the PDO is also associated with strong tropical Pacific SST anomalies (Zhang et al. 1997) and these PDO–hydroclimate links could be explained by the tropical SST anomalies. Indeed, no GCM study to date has demonstrated that any appreciable portion of the hydroclimate history of North America is explained as a response to extratropical SST anomalies either in the Pacific or Atlantic Oceans. It is worth noting, however, that Fye et al. (2004) surmised the atmospheric circulation anomalies during the pluvial using only North Pacific SST information, conjecturing that the combined warm tropical Pacific and cold North Pacific would lead to anticyclonic anomalies over the western North Pacific and a long-wave trough centered near the west coast of NA. While the physical basis for why this would happen is unclear, these circulation features are clearly shown in Fig. 11. It may be that this GCM, like others, potentially misses an impact of SST anomalies in the extratropical Pacific on hydroclimatic variability over NA (which are implicitly resolved within a statistical framework) or it could be that the circulation anomalies important to the pluvial were a combination of El Niño forcing with significant

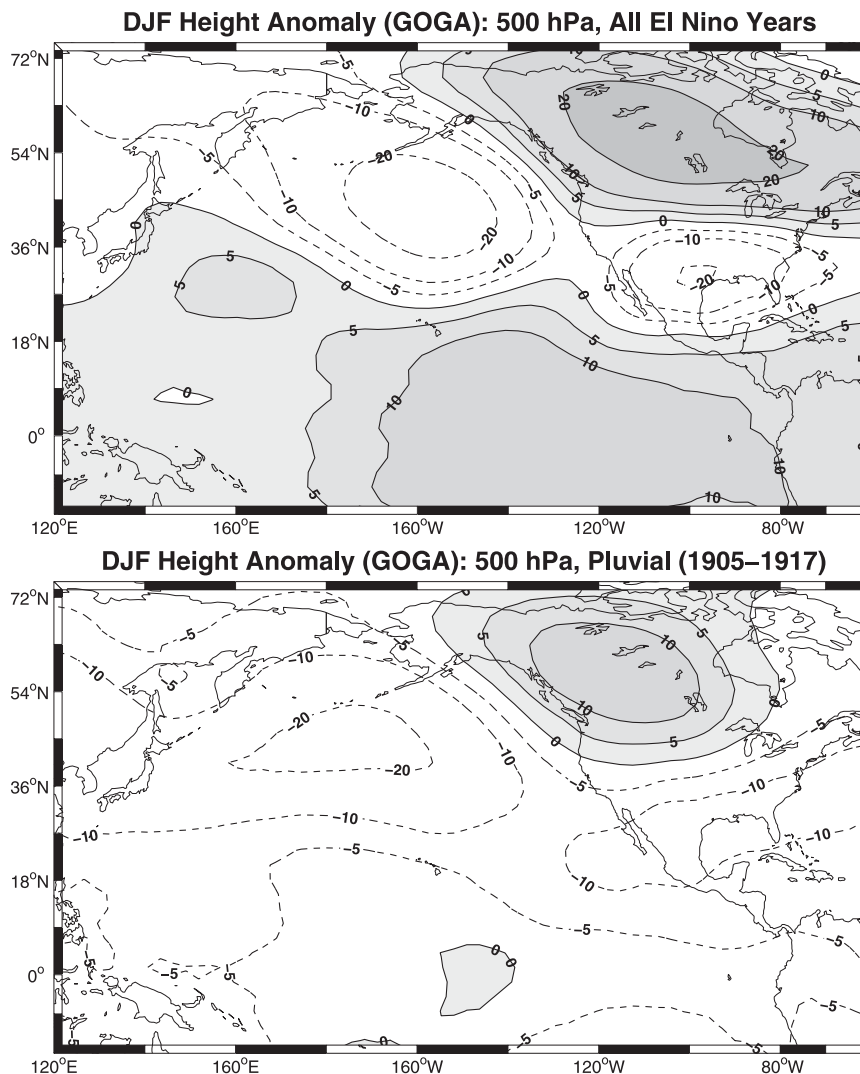


FIG. 13. Composite 500-hPa geopotential heights (m) for (top) all El Niño years and (bottom) all pluvial years (1905–17) from the ensemble mean of the GCM simulations.

internal atmospheric variability, such as the AO. Only more work, including simulation with other GCMs, may be able to resolve this issue.

4. Conclusions

Throughout history, persistent periods of extreme climate have significantly impacted the functioning of societies, and have often been instrumental in shaping resource use policies and societal reorganizations (e.g., Buckley et al. 2010; Hansen and Libecap 2004). One such event, the early twentieth-century pluvial, set up unrealistic expectations for water availability in western NA, leading to development trajectories that surpassed the long-term support capacity defined by the climatology of the region

(Christensen et al. 2004). Increasing our understanding of the causes and dynamics of this, and other, climate events can help us place current and future climate changes in the proper context and inform how we deal with these events at the societal level. The specific goal of this study was to investigate the causes of the moisture surpluses during the early twentieth-century pluvial and to determine how well anomalies during that time fit into our understanding of NA hydroclimatic variability. Our main results are summarized:

- Across the West, the origin of the moisture surpluses during the pluvial varied by region and can be attributed primarily to increased precipitation (the SW), decreased evaporative demand (the CP), or a combination of the two (the NW).

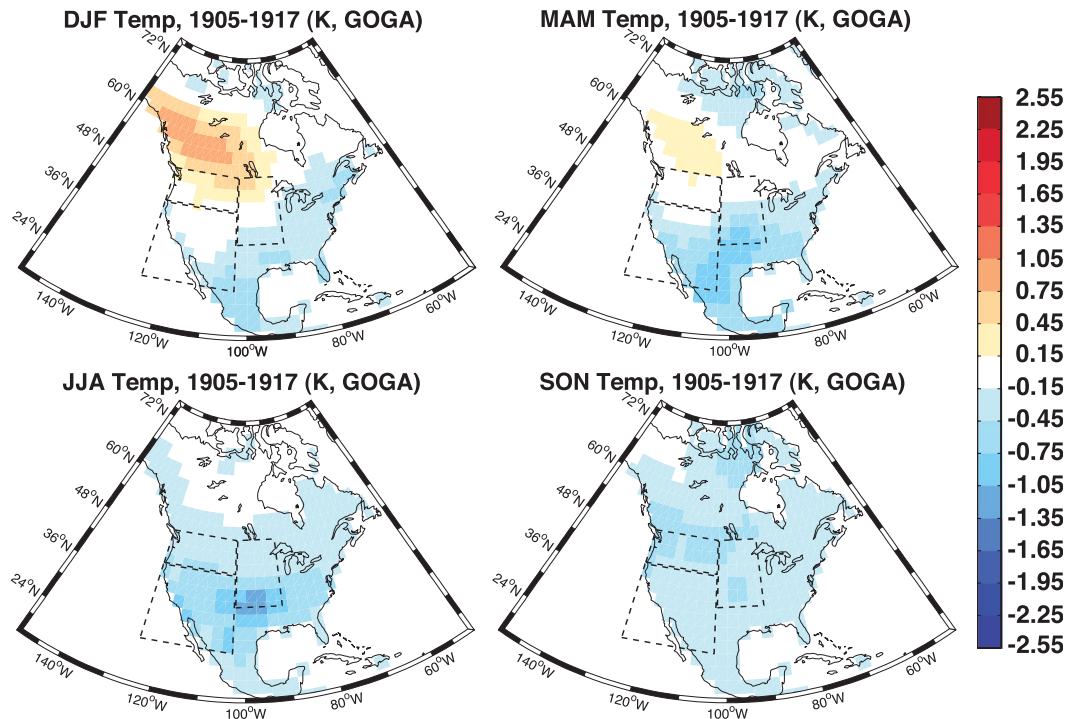


FIG. 14. Temperature anomalies during 1905–17 from the ensemble mean of the GCM simulations (K), relative to the 1961–90 ensemble mean.

- El Niño played a partial role in the pluvial circulation anomalies and moisture surpluses, contributing primarily to increased moisture convergence and precipitation in the SW. However, other anomalies in the SST, circulation, and precipitation anomaly fields diverged from the expected El Niño response. Forced circulation responses to cold extratropical SSTs in the North Pacific were difficult to definitively diagnose either within the 20CR or the GOGA model runs.
- Ten winters during the pluvial were associated with +AO events, and this is reflected in much of the circulation, temperature, and precipitation anomaly patterns during DJF. The large role played by the AO, an internal mode of atmospheric variability, coupled with the relatively weak ENSO and SST forcing at the time, implies that the pluvial was not predictable from SST information. If, however, the AO continues along a positive trajectory, as predicted by many models (Miller et al. 2006), it may help ameliorate some of the projected drying in the subtropics, including the SW region (Seager 2007).
- However, the intensity and spatial extent of the pluvial can be well reproduced using a statistical model with conceptualized tropical and extratropical Pacific SST forcings (Cook et al. 2011a). An independent GCM simulation driven by SST observations produces the

El Niño response observed during the pluvial but is incapable of simulating other important features.

Studies of pluvial events (e.g., Schubert et al. 2008; Seager et al. 2005b) in the climate literature are relatively rare when compared to the wealth of drought investigations. This asymmetry is somewhat understandable, given the huge direct and indirect economic costs associated with droughts (e.g., Cook et al. 2007). Even climatically advantageous periods like the pluvial, however, may have adverse consequences if they are not placed within the proper context, as witnessed by the overly generous nature of the CRC (Christensen et al. 2004). Extensive research into drought variability over North America has helped illuminate the role of SST variability in the ENSO region, and highlighted the importance of La Niña events as major drivers of persistent drought in the West (e.g., Seager et al. 2005b). For the early twentieth-century pluvial, however, our investigation indicates that SSTs in the ENSO region had relatively little explanatory power and highlights the potentially important role of internal variability (the AO, cool temperatures, etc) for driving moisture surpluses. Research into pluvial dynamics is hampered, however, by the paucity of extended pluvial events that have occurred during the instrumental period.

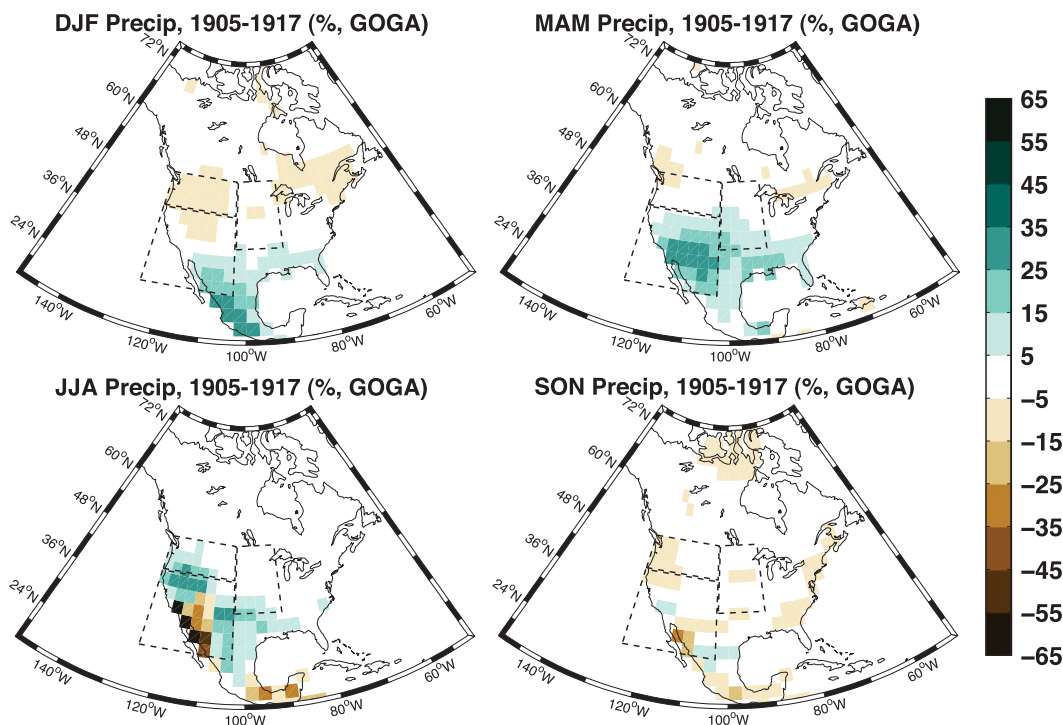


FIG. 15. Precipitation anomalies during 1905–17 from the ensemble mean of the GCM simulations, expressed as a percent difference relative to the 1961–90 ensemble mean.

The discrepancy between the statistical model and the GCM also highlights some of the uncertainties and the often disparate conclusions reached by empirical (McCabe et al. 2004, 2008) versus model-based (Seager et al. 2005b; Seager 2007) investigations of North American hydroclimatic variability. Specifically, the two camps disagree on the efficacy of extratropical North Pacific forcing of NA hydroclimate with the GCM experiments indicating the dominance of tropical forcing. Reducing this key uncertainty will require further studies exploiting both empirical analyses and modeling.

Acknowledgments. The authors thank three anonymous reviews for comments that significantly improved the quality of this manuscript. Twentieth Century Reanalysis V2 data were provided by the NOAA/OAR/ESRL PSD, Boulder, Colorado, from their Web site (<http://www.esrl.noaa.gov/psd/>). Support for the Twentieth Century Reanalysis Project dataset is provided by the U.S. Department of Energy, Office of Science Innovative and Novel Computational Impact on Theory and Experiment (DOE INCITE) program, and the Office of Biological and Environmental Research (BER), and by the National Oceanic and Atmospheric Administration Climate Program Office. The authors gratefully acknowledge support from the NSF Grant ATM-06-20066 and the NASA Atmospheric Composition Program,

as well as NSF Grant ATMO9-02716, NOAA Award NA08OAR4320912, and NOAA Grant NA10OAR-4310137.

REFERENCES

- Adams, D., and A. Comrie, 1997: The North American monsoon. *Bull. Amer. Meteor. Soc.*, **78**, 2197–2213.
- An, S., J. Kug, A. Timmermann, I. Kang, and O. Timm, 2007: The influence of ENSO on the generation of decadal variability in the North Pacific. *J. Climate*, **20**, 667–680.
- Andrade, E., Jr., and W. Sellers, 1988: El Niño and its effect on precipitation in Arizona and western New Mexico. *Int. J. Climatol.*, **8**, 403–410.
- Barnett, T., and D. Pierce, 2009: Sustainable water deliveries from the Colorado River in a changing climate. *Proc. Natl. Acad. Sci. USA*, **106**, 7334.
- Brohan, P., J. Kennedy, I. Harris, S. Tett, and P. Jones, 2006: Uncertainty estimates in regional and global observed temperature changes: A new data set from 1850. *J. Geophys. Res.*, **111**, D12106, doi:10.1029/2005JD006548.
- Buckley, B., and Coauthors, 2010: Climate as a contributing factor in the demise of Angkor, Cambodia. *Proc. Natl. Acad. Sci. USA*, **107**, 6748–6752, doi:10.1073/pnas.0910827107.
- Christensen, N., A. Wood, N. Voisin, D. Lettenmaier, and R. Palmer, 2004: The effects of climate change on the hydrology and water resources of the Colorado River basin. *Climatic Change*, **62**, 337–363.
- Compo, G., J. Whitaker, and P. Sardeshmukh, 2006: Feasibility of a 100-year reanalysis using only surface pressure data. *Bull. Amer. Meteor. Soc.*, **87**, 175–190.

- , and Coauthors, 2011: The Twentieth Century Reanalysis Project. *Quart. J. Roy. Meteor. Soc.*, **137**, 1–28, doi:10.1002/qj.776.
- Cook, B., E. Cook, K. Anchukaitis, R. Seager, and R. Miller, 2011a: Forced and unforced variability of twentieth century North American droughts and pluvials. *Climate Dyn.*, **37**, 1097–1110, doi:10.1007/s00382-010-0897-9.
- , R. Seager, and R. Miller, 2011b: Atmospheric circulation anomalies during two persistent North American droughts: 1932–1939 and 1948–1957. *Climate Dyn.*, **36**, 2339–2355, doi:10.1007/s00382-010-0807-1.
- Cook, E., D. Meko, D. Stahle, and M. Cleaveland, 1999: Drought reconstructions for the continental United States. *J. Climate*, **12**, 1145–1162.
- , C. Woodhouse, C. Eakin, D. Meko, and D. Stahle, 2004: Long-term aridity changes in the western United States. *Science*, **306**, 1015–1018.
- , R. Seager, M. Cane, and D. Stahle, 2007: North American drought: Reconstructions, causes, and consequences. *Earth Sci. Rev.*, **81**, 93–134.
- Deser, C., M. Alexander, S. Xie, and A. Phillips, 2010: Sea surface temperature variability: Patterns and mechanisms. *Annu. Rev. Mater. Sci.*, **2**, 115–143.
- Dettinger, M., 2004: Fifty-two years of “pineapple-express” storms across the West Coast of North America. PIER Project Rep., California Energy Commission Rep. CEC-500-2005-004, 15 pp. [Available online at <http://www.energy.ca.gov/2005publications/CEC-500-2005-004/CEC-500-2005-004.PDF>.]
- Dracup, J., K. Lee, and E. Paulson Jr., 1980: On the definition of droughts. *Water Resour. Res.*, **16**, 297–302.
- Enfield, D., A. Mestas-Nunez, and P. Trimble, 2001: The Atlantic multidecadal oscillation and its relationship to rainfall and river flows in the continental US. *Geophys. Res. Lett.*, **28**, 2077–2080.
- Frankignoul, C., and N. Sennéchal, 2007: Observed influence of North Pacific SST anomalies on the atmospheric circulation. *J. Climate*, **20**, 592–606.
- Fye, F., D. Stahle, and E. Cook, 2003: Paleoclimatic analogs to twentieth-century moisture regimes across the United States. *Bull. Amer. Meteor. Soc.*, **84**, 901–909.
- , —, and —, 2004: Twentieth-century sea surface temperature patterns in the Pacific during decadal moisture regimes over the United States. *Earth Interact.*, **8**, 1–22. [Available online at <http://EarthInteractions.org>.]
- Gershunov, A., and T. Barnett, 1998: Interdecadal modulation of ENSO teleconnections. *Bull. Amer. Meteor. Soc.*, **79**, 2715–2725.
- Goodrich, G., 2007: Influence of the Pacific decadal oscillation on winter precipitation and drought during years of neutral ENSO in the western United States. *Wea. Forecasting*, **22**, 116–124.
- Hansen, Z., and G. Libecap, 2004: Small farms, externalities, and the Dust Bowl of the 1930s. *J. Polit. Econ.*, **112**, 665–694.
- Herweijer, C., R. Seager, E. Cook, and J. Emile-Geay, 2007: North American droughts of the last millennium from a gridded network of tree-ring data. *J. Climate*, **20**, 1353–1376.
- Hobbins, M., A. Dai, M. Roderick, and G. Farquhar, 2008: Revisiting the parameterization of potential evaporation as a driver of long-term water balance trends. *Geophys. Res. Lett.*, **35**, L12403, doi:10.1029/2008GL033840.
- Hu, Q., and S. Feng, 2010: Influence of the Arctic oscillation on central United States summer rainfall. *J. Geophys. Res.*, **115**, D01102, doi:10.1029/2009JD011805.
- Junge, M., and T. Haine, 2001: Mechanisms of North Atlantic wintertime sea surface temperature anomalies. *J. Climate*, **14**, 4560–4572.
- Kalnay, E., and Coauthors, 1996: The NCEP/NCAR 40-Year Reanalysis Project. *Bull. Amer. Meteor. Soc.*, **77**, 437–471.
- Kaplan, A., M. Cane, Y. Kushnir, A. Clement, M. Blumenthal, and B. Rajagopalan, 1998: Analyses of global sea surface temperature 1856–1991. *J. Geophys. Res.*, **103**, 18 567–18 589.
- Kiehl, J., J. Hack, G. Bonan, B. Boville, D. Williamson, and P. Rasch, 1998: The National Center for Atmospheric Research Community Climate Model: CCM3. *J. Climate*, **11**, 1131–1149.
- Kurtzman, D., and B. Scanlon, 2007: El Niño–Southern Oscillation and Pacific decadal oscillation impacts on precipitation in the southern and central United States: Evaluation of spatial distribution and predictions. *Water Resour. Res.*, **43**, W10427, doi:10.1029/2007WR005863.
- Kushnir, Y., W. Robinson, I. Blade, N. Hall, S. Peng, and R. Sutton, 2002: Atmospheric GCM response to extratropical SST anomalies: Synthesis and evaluation. *J. Climate*, **15**, 2233–2256.
- , R. Seager, M. Ting, N. Naik, and J. Nakamura, 2010: Mechanisms of tropical Atlantic SST influence on North American hydroclimate variability. *J. Climate*, **23**, 5610–5628.
- MacDonnell, L., D. Getches, and W. Hugenberg Jr., 1995: The law of the Colorado River: Coping with severe sustained drought. *Water Resour. Bull.*, **31**, 825–836.
- Mantua, N., S. Hare, Y. Zhang, J. Wallace, and R. Francis, 1997: A Pacific interdecadal climate oscillation with impacts on salmon production. *Bull. Amer. Meteor. Soc.*, **78**, 1069–1079.
- McAfee, S., and J. Russell, 2008: Northern annular mode impact on spring climate in the western United States. *Geophys. Res. Lett.*, **35**, L17701, doi:10.1029/2008GL034828.
- McCabe, G., M. Palecki, and J. Betancourt, 2004: Pacific and Atlantic Ocean influences on multidecadal drought frequency in the United States. *Proc. Natl. Acad. Sci. USA*, **101**, 4136–4141.
- , J. Betancourt, S. Gray, M. Palecki, and H. Hidalgo, 2008: Associations of multi-decadal sea-surface temperature variability with US drought. *Quat. Int.*, **188**, 31–40.
- Meko, D., C. Woodhouse, C. Baisan, T. Knight, J. Lukas, M. Hughes, and M. Salzer, 2007: Medieval drought in the upper Colorado River basin. *Geophys. Res. Lett.*, **34**, 10 705–10 709.
- Miller, R., G. Schmidt, and D. Shindell, 2006: Forced annular variations in the 20th century Intergovernmental Panel on Climate Change Fourth Assessment Report models. *J. Geophys. Res.*, **111**, D18101, doi:10.1029/2005JD006323.
- Mitchell, T., and P. Jones, 2005: An improved method of constructing a database of monthly climate observations and associated high-resolution grids. *Int. J. Climatol.*, **25**, 693–712.
- Mo, K., J. Schemm, and S. Yoo, 2009: Influence of ENSO and the Atlantic multidecadal oscillation on drought over the United States. *J. Climate*, **22**, 5962–5982.
- Palmer, W. C., 1965: Meteorological drought. U.S. Weather Bureau Research Paper 45, 58 pp. [Available online at <http://www.ncdc.noaa.gov/temp-and-precip/drought/docs/palmer.pdf>.]
- Peng, S., and J. Whitaker, 1999: Mechanisms determining the atmospheric response to midlatitude SST anomalies. *J. Climate*, **12**, 1393–1408.
- Rayner, N., D. Parker, E. Horton, C. Folland, L. Alexander, D. Rowell, E. Kent, and A. Kaplan, 2003: Global analyses of sea surface temperature, sea ice, and night marine air temperature since the late nineteenth century. *J. Geophys. Res.*, **108**, 4407, doi:10.1029/2002JD002670.
- Reisner, M., 1993: *Cadillac Desert: The American West and Its Disappearing Water*. Penguin Group, 582 pp.

- Schneider, N., and B. Cornuelle, 2005: The forcing of the Pacific decadal oscillation. *J. Climate*, **18**, 4355–4373.
- Schubert, S., M. Suarez, P. Pegion, R. Koster, and J. Bacmeister, 2008: Potential predictability of long-term drought and pluvial conditions in the U.S. Great Plains. *J. Climate*, **21**, 802–816.
- , and Coauthors, 2009: A U.S. CLIVAR project to assess and compare the responses of global climate models to drought-related SST forcing patterns: Overview and results. *J. Climate*, **22**, 5251–5272.
- Seager, R., 2007: The turn-of-the-century North American drought: Global context, dynamics, and past analogs. *J. Climate*, **20**, 5527–5552.
- , N. Harnik, Y. Kushnir, W. Robinson, and J. Miller, 2003: Mechanisms of hemispherically symmetric climate variability. *J. Climate*, **16**, 2960–2978.
- , —, W. Robinson, Y. Kushnir, M. Ting, H. Huang, and J. Velez, 2005a: Mechanisms of ENSO-forcing of hemispherically symmetric precipitation variability. *Quart. J. Roy. Meteor. Soc.*, **131**, 1501–1527.
- , Y. Kushnir, C. Herweijer, N. Naik, and J. Velez, 2005b: Modeling of tropical forcing of persistent droughts and pluvials over western North America: 1856–2000. *J. Climate*, **18**, 4065–4088.
- Sophocleous, M., 2010: Groundwater management practices, challenges, and innovations in the High Plains aquifer, USA—Lessons and recommended actions. *Hydrogeol. J.*, **18**, 559–575.
- St. George, S., D. Meko, and E. Cook, 2010: The seasonality of precipitation signals embedded within the North American Drought Atlas. *Holocene*, **20**, 983–988.
- Stockton, C. W., and G. C. Jacoby Jr., 1976: Long-term surface-water supply and streamflow trends in the Upper Colorado River basin based on tree-ring analysis. Lake Powell Research Project Bull. 1, 70 pp. + viii. [Available online at <http://www.gcmrc.gov/library/reports/physical/hydrology/Stockton1976.pdf>.]
- Thompson, D., and J. Wallace, 1998: The Arctic Oscillation signature in the wintertime geopotential height and temperature fields. *Geophys. Res. Lett.*, **25**, 1297–1300.
- Thorntwaite, C., 1948: An approach toward a rational classification of climate. *Geogr. Rev.*, **38**, 55–94.
- Wallace, J., and D. Gutzler, 1981: Teleconnections in the geopotential height field during the Northern Hemisphere winter. *Mon. Wea. Rev.*, **109**, 784–812.
- Wen, N., Z. Liu, Q. Liu, and C. Frankignoul, 2010: Observed atmospheric responses to global SST variability modes: A unified assessment using GEFA. *J. Climate*, **23**, 1739–1759.
- Whitaker, J., G. Compo, X. Wei, and T. Hamill, 2004: Reanalysis without radiosondes using ensemble data assimilation. *Mon. Wea. Rev.*, **132**, 1190–1200.
- Wood, K., and J. Overland, 2009: Early 20th century Arctic warming in retrospect. *Int. J. Climatol.*, **30**, 1269–1279, doi:10.1002/joc.1973.
- Woodhouse, C., K. Kunkel, D. Easterling, and E. Cook, 2005: The twentieth-century pluvial in the western United States. *Geophys. Res. Lett.*, **32**, L07701, doi:10.1029/2005GL022413.
- Worster, D., 1992: *Rivers of Empire: Water, Aridity, and the Growth of the American West*. Oxford University Press, 402 pp.
- Zhang, Y., J. Wallace, and D. Battisti, 1997: ENSO-like interdecadal variability: 1900–93. *J. Climate*, **10**, 1004–1020.